

Scientific paper

Infrared Spectroscopic and Conductivity Studies of Ureasil-Based Proton Conducting Membranes for Medium Temperature Fuel Cell Applications

Jelica Vince,¹ Angela Šurca Vuk,¹ Urška Lavrenčič Štangar,²
Lidija Slemenik Perše,¹ Boris Orel^{1,*} and Stanko Hočevar¹

¹ National Institute of Chemistry, Hajdrihova 19, SI-1000 Ljubljana, Slovenia

² University of Nova Gorica, Vipavska 13, SI-5000 Nova Gorica, Slovenia

* Corresponding author: E-mail: boris.orel@ki.si

Tel.: 00386-(0)1-4760-276; 00386-(0)1-4760-300

Received: 14-04-2010

Abstract

Proton conducting membranes for fuel cells were prepared by the sol-gel process from two different ureasil organic-inorganic hybrid precursors: bis[*N*-(3-triethoxysilylpropyl)ureido]-terminated poly(propylene glycol) 4000 (PPGU) and bis[3-(*N*-(3-triethoxysilylpropyl)ureido)propyl]-terminated poly(dimethylsiloxane) 1000 (PDMSU). Heteropoly silicotungstic acid was added to actuate the reactions of hydrolysis and condensation and to introduce proton conductivity. XRD measurements of membranes revealed the presence of a diffraction peak at 6.3°, which could be ascribed to gradual formation of R-(SiO_{3/2}) silsesquioxane clusters, i.e. arrangement of the Si-O-Si skeleton on the nano-scale. TG and DSC measurements showed thermal stability of the membranes above 120 °C. Proton conductivities at room temperature were of the order of 10⁻⁴ to 10⁻³ S/cm, classifying the membranes in the group of super ionic conductors. At elevated temperatures up to 160 °C and at conditions of autogenous pressure, conductivities increased up to values acceptable for fuel cells of 10⁻¹ S/cm, which could be the result of the presence of H₃O⁺ ions. The protonation of the urea groups and the formation of amidonium ions [C(OH)=NH⁺] were followed using IR ATR spectroscopy.

Keywords: Proton-conducting membranes, organically modified silanes, sol-gel, heteropoly acid, fuel cells.

1. Introduction

Fuel cells represent an important and growing field of research which is driven by the need to find energy with negligible pollutant emissions. Polymer proton conducting membrane fuel cells use as fuel either pure hydrogen or hydrogen derived from fossil fuels or alcohol. Nowadays, proton exchange membrane fuel cells (PEMFC) are mostly composed of perfluorosulfonic polymer membranes like Nafion.^{1,2} These membranes exhibit high proton conductivity and chemical stability, but in addition to their high cost, they are insufficiently stable for temperature operation above 90 °C. The major challenge is therefore to find a polymer membrane with a higher temperature stability. Besides, the membrane also has to fulfil other basic requirements: it should be a good proton conductor, electrically non-conductive, permeable

to reactant gases (hydrogen, oxygen), while impermeable to water molecules.

The syntheses of materials using sol-gel procedures^{3,4} have recently gained in importance mainly, due to the mild synthesis conditions and the possibility of tailoring the desired product properties on the molecular scale. Nanocomposite materials in particular are becoming prominent for their outstanding properties and are used in technologically highly developed systems and devices. Nanocomposite materials are prepared from hybrid organic-inorganic precursors, i.e. various organically modified alkoxysilanes,⁵ which under certain conditions crosslink and form materials with elasticity, hardness and also appropriate thermal stability. The organic part of the hybrid precursor imparts flexibility and elasticity to the material, while the inorganic part provides mechanical and chemical stability, as well as dimen-

sional and thermal stability. In sol-gel proton conducting membranes^{6–12} high amounts of hydrogen (H^+) ions can be incorporated, leading to their highly conducting properties. As a source of hydrogen ions H^+ heteropoly acids are usually used, mostly either phosphotungstic acid (PWA)^{13–16} or silicotungstic acid (SiWA),^{16–19} which are both super ionic conductors at room temperature.

The present study is a continuation of our previous work²⁰ on the development of new nanocomposite membranes with high SiWA content, which provide a proton conductivity between 10^{-5} and 10^{-3} S/cm at room temperature. We have focused on nanocomposite materials which are stable at elevated temperatures in the range of 100–160 °C.^{21–23} The synthesis of optically transparent and homogeneous gels and membranes was performed via the hydrolysis and condensation reactions of the alkoxy groups of hybrid organic-inorganic precursors, which contained either poly(propylene glycol) (PPGU)²⁴ or poly(dimethylsiloxane) (PDMSU) chains. Both hybrid precursors belong to class II precursors,²⁵ where the organic and inorganic parts of the molecule are covalently bonded. The precursors used in this study are structurally similar to ureasils, since the covalent bond is formed

through formation of urea groups. The prepared series of gels and membranes contained different amounts of heteropoly acid (SiWA). The commercial silanes phenyltriethoxysilane (PhTEOS) and 1*H*,1*H*,2*H*,2*H*-perfluorooctyltriethoxysilane (PFOTEOS) were used as network modifiers for optimizing the time of gelation, mechanical properties, ionic conductivity and retention of the acid in the membrane. Our aim was to prepare hydrophobic membranes (no swelling in water) with low leaching of the acid in order to retain a proton conductivity high enough for fuel cell application.

The structural properties of the prepared membranes were investigated using XRD and IR spectroscopy. The latter technique was used to prove the presence of proton species, i.e. H_3O^+ ions as the charge carriers and amidonium ions ($[C(OH)=NH^+]$),²⁶ which formed in the presence of higher amount of a SiWA. The evolution of bands characteristic of $[C(OH)=NH^+]$ and H_3O^+ species was correlated to the changes in proton conductivity at different temperatures. The thermal stability of the proton conducting membranes and their possible application in fuel cells operating at temperatures up to 160 °C, was investigated using thermogravimetric (TG) measurements.

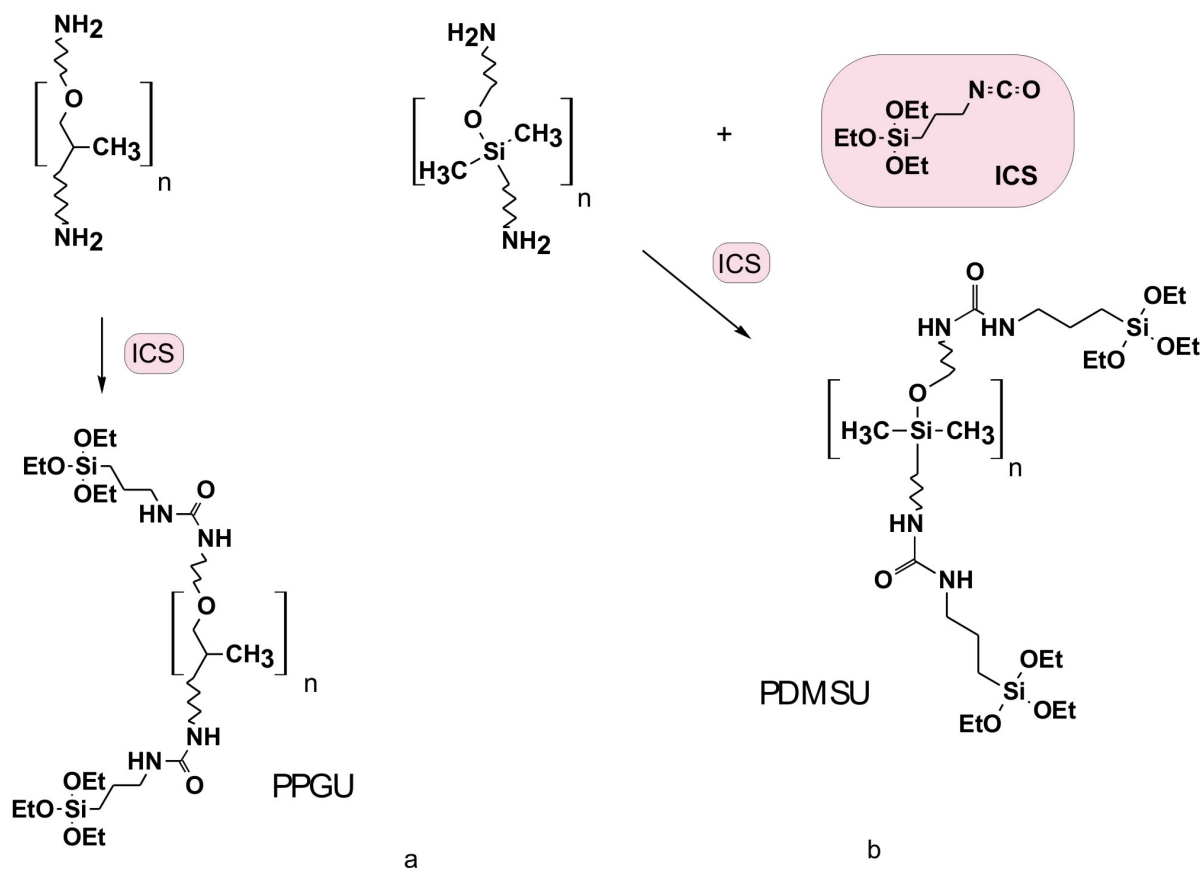


Fig. 1: Synthesis of organic-inorganic hybrid precursors: a) bis[*N*-(3-triethoxysilylpropyl)ureido]-terminated poly(propylene glycol) 4000 (PPGU) and b) bis[3-(*N*-(3-triethoxysilylpropyl)ureido)propyl]-terminated poly(dimethylsiloxane) 1000 (PDMSU).

2. Experimental

2. 1. Synthesis of Di-Ureasils

Two organic-inorganic hybrid precursors were prepared using the acylation reaction between amino and isocyanato groups:²⁵

- bis[*N*-(3-triethoxysilylpropyl)ureido]-terminated poly(propylene glycol) 4000 (PPGU),
- bis[3-(*N*-(3-triethoxysilylpropyl)ureido)propyl]-terminated poly(dimethylsiloxane) 1000 (PDM-SU).

These hybrid precursors belong to the class of ureasils, which are characterized by urea groups connecting a polymer chain of either poly(propylene glycol) (Fig. 1a) or poly(dimethylsiloxane) (Fig. 1b) with two terminal alkyltrialkoxysilane groups. The details of the synthesis were reported in our previous publication.²⁰

2. 2. Preparation of Membranes

Membranes were prepared from two different network formers, i.e. hybrid PPGU and PDMSU precursors, which were first diluted in ethanol. As network modifiers were then added PFOTEOS (ABCR), PhTEOS (ABCR) or surfactant Brij 56 (Aldrich), the latter with chemical formula $C_{16}H_{33}(OCH_2CH_2)_nOH$, $n \approx 10$ (polyoxyethylene (10) cetyl ether). After vigorous stirring a clear solution was obtained into which the solution of silicotungstic acid $H_4SiW_{12}O_{40} \cdot nH_2O$ (SiWA) in ethanol was added and stirred until homogenization of the sol.

The membranes were prepared by casting the fresh sol in a Teflon dish (diameter 9 cm), where it gelled and solidified, usually within 24 h, when the ethanol completely evaporated. Membranes thinner than 100 μm were prepared by drawing the sol on a flexible Teflon substrate. The compositions of the investigated membranes are shown in Table 1.

Table 1: Composition of membranes prepared from PPGU and PDMSU network formers.

Type	Network former		Network modifier		Acid SiWA	
	<i>m</i> [g]	Type	<i>m</i> [g]	Type	<i>m</i> [g]	%SiWA [%]
A	0.5	PPGU	0.34	PFOTEOS	0.69	40
B	0.5	PDMSU	0.26	Brij 56	0.41	31
C	0.5	PDMSU	0.033	PhTEOS	0.60	36
	0.33	PPGU				
D	0.5	PPGU	0.32	PhTEOS	0.69	40

The content of SiWA in the membranes was defined as the mass ratio between the mass of SiWA (without hydrate water as defined from thermogravimetric measurements) and the sum of the masses of SiWA acid hydrate (m_{SiWA}), network formers (m_{NF}) and network mo-

differs (m_{NM}):

$$\%SiWA = \frac{m_{SiWA(\text{without hydrate water})}}{(m_{SiWA} + m_{NF} + m_{NM})} \cdot 100 [\%] \quad (1)$$

The membranes were made with %SiWA = 20–80%. The %SiWA shown in Table 1 was used unless otherwise stated in text.

2. 3. Measurement Techniques for the Characterization of Membranes

IR spectra were measured using a Bruker Model IFS 66/S spectrometer with a resolution of 4 cm^{-1} in the spectral range of 4000–400 cm^{-1} . Various sol-gel membranes were investigated by IR ATR spectra measurements using a horizontal Silver Gate ATR cell (angle of incidence 45°), equipped with a Ge ATR crystal ($n = 4$). The membranes were then equilibrated in an autoclave at temperatures up to 160 °C and the autogenous water pressure, and the IR ATR spectra of the treated membranes were then measured at ambient conditions (ex-situ IR ATR spectroscopy).

Impedance measurements of resistance (R) were performed at room temperature using a 1286 Solartron Electrochemical Interface and a 1250 Solartron Frequency Response Analyser. The impedance spectra were recorded in the range of 65000 and 0.001 Hz. Two types of measurements were performed: (i) in situ measurements of electrolytes in the course of gelling in a vessel; (ii) measurements of membranes, cast and dried on Teflon dishes. The conductivity measurement of gels (i) was made using two parallel glassy plates, coated with a conducting $SnO_2 : F$ layer. In order to ensure good contact, the electrodes were dipped into the sol before gelling. The distance between the electrodes was 0.3 cm and the active surface of the electrodes in contact with the electrolyte was from 0.8–1.5 cm^2 (the exact value was determined individually for each sample). The resistance of the electrodes R_e was 101.4 Ω and was determined by pasting them with silver paste of negligible resistance. The ionic conductivity was calculated by the following equation:

$$\sigma = \frac{d}{(R_m - R_e) \cdot A} \quad [S/cm] \quad (2)$$

where d is the distance between the electrodes, R_m is the measured resistance of the membrane, R_e is the resistance of the electrodes and A is the active surface of the electrodes in contact with the electrolyte. The impedance measurements of membranes (ii) in the temperature range between 25 and 160 °C were performed in a “zero-gap” type autoclave cell. The heating rate was 2 °/min at the conditions of autogenous water pressure. The resistance at each temperature step was measured after at least 15 min of equilibration time. An HP 4284A LCR Meter with Kelvin

clamps and HP VEE OneLab software were used to measure the resistance at 1 kHz alternating current.

Measurements of X-ray diffraction (XRD) of the membranes were performed using a Philips PW1710 automatic X-ray diffractometer with $\text{CuK}\alpha$, $\lambda = 0.154$ nm monochromatic radiation using a $2\theta = 0.025^\circ$ step. The time of recording of an XRD patterns at a particular angle was 1 s.

Thermogravimetric measurements (TG) of membranes and precursors were made on a DSC-TGA SDT 2960 (TA Instrument, New Castle, USA) using a $10^\circ/\text{min}$ temperature ramp under static air.

3. Results and Discussion

3.1. Thermal Properties: TG and DSC Measurements

The thermal stability of the precursors and membranes was tested by employing TG and DSC measurements. The TG measurements of precursors revealed that their weight loss was less than 2% up to 120°C , but increased to 5% for PDMSU and 10% for PPGU in the temperature region between 160 and 200°C . Above 200°C thermal decomposition of PPGU occurred rapidly and almost 90% of the initial mass decomposed up to 300°C , while the weight loss was much slower for PDMSU (at 300°C , less than 25% of the initial mass was lost) due to the presence of poly(dimethylsiloxane) chains.

Membrane A: TG analysis of membrane A (Fig. 2) revealed a weight loss of only 1.6% up to 100°C , which we attributed to the loss of acid water. The dehydration process was confirmed by DSC measurements showing an endothermic peak at 50°C . Up to 170°C the weight loss of membrane A increased significantly due to decomposition of the organic part of the poly(propylene glycol) chains.

Membrane B: The weight loss of this membrane (Fig. 2) occurred in two steps and was of lower rate as

compared to membrane A. Up to 125°C the weight loss could be ascribed to dehydration, while at temperatures above 250°C the thermal decomposition stemmed from degradation of the organic groups in PDMSU and Brij 56 surfactant (Table 1). The latter decomposed first as could be inferred by comparing the DSC curves of the precursor PDMSU and the membrane B. At higher temperatures the decomposition process became complex due to the stability of the poly(dimethylsiloxane) chains, which gradually transformed into the more thermally stable siloxane network. However, the corresponding temperature range was not relevant for this work.

Membrane C: Expectedly, the TG behaviour of membrane C (Fig. 2) was similar to that of membrane B due to the similarity in their structures. However, up to 120°C the weight loss was lower than for membrane B. At temperatures above 150°C the weight loss was faster compared to membrane B, probably due to the degradation of poly(propylene glycol) chains, which were not present in membrane B. However, above 290°C membrane C started to decompose but not as fast as membrane B, indicating the synergetic effect of the presence of poly(propylene glycol) and poly(dimethylsiloxane) chains in the sol-gel network. Nevertheless, the stabilisation effect of the poly(dimethylsiloxane) in the PPGU network was evident.

In the temperature interval up to 160°C , in which the proton conductivity was also investigated, membrane C showed the highest thermal stability followed by membrane B.

3.2. XRD Measurements of Membranes A, B, C

The XRD measurements were performed to provide insight into the long range ordering effect in sol-gel materials stemming from the formation of cyclic (T^2 in ^{29}Si NMR spectra), open polyhedral and cube-like (T^3) species, the latter typical of the silsesquioxane ($(\text{R}-\text{SiO}_{3/2})_n$) species. All membranes showed similar XRD patterns (Fig. 3A) characterized by low-intensity peaks at $\approx 20^\circ$,

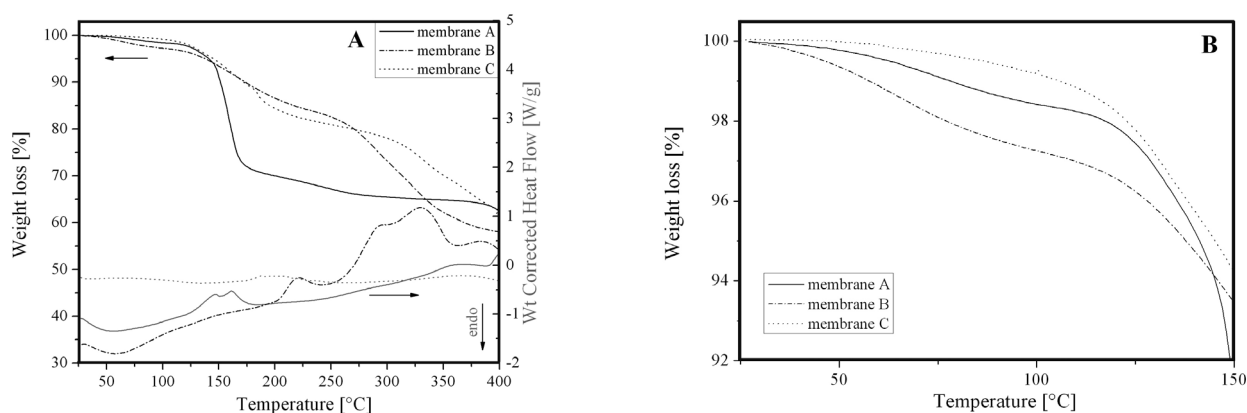


Fig. 2: TG and DSC curves of the membranes A, B and C: A) 25–400 °C and B) 25–150 °C.

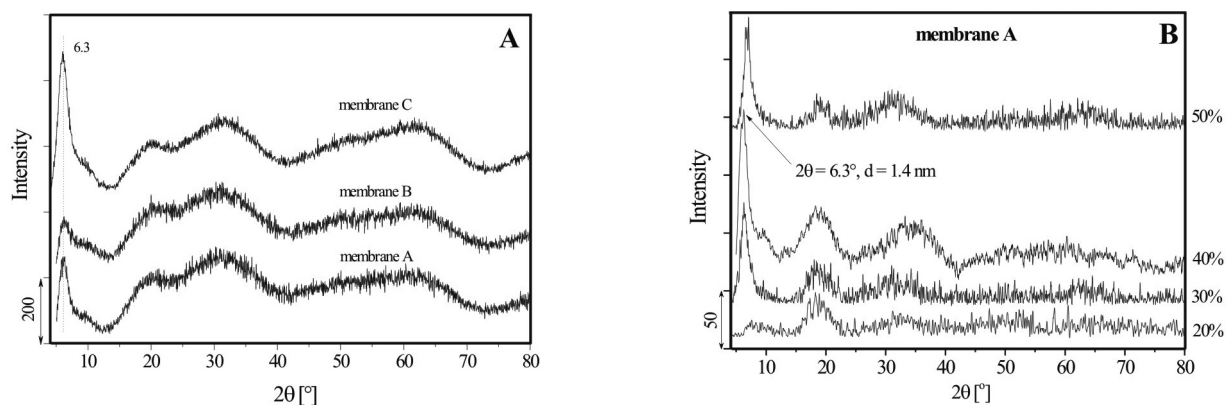


Fig. 3: XRD patterns of: A) membranes A, B and C and B) membrane A with different contents of SiWA acid.

$\approx 30^\circ$ and $\approx 62^\circ$. The broad diffraction peak at $\approx 20^\circ$ was attributed to structural arrangement of the silica units on a nano scale²⁷ by analogy with the XRD patterns of other alkylalkoxysilane gels and xerogels.²⁸ The most important diffraction peak was found at $2\theta = 6.3^\circ$, ascribed to the presence of adjacent $(R-SiO_{3/2})_n$ clusters of polyhedral silsesquioxanes, also noted for example in methyltriethoxysilane (MTEOS) gels at $2\theta = 10^\circ$.^{29,30} The appearance of the corresponding peak at lower 2θ angles was expected due to the presence of large R-groups in the membranes, in comparison to MTEOS where $R = -CH_3$.^{31,32}

It should be stressed that the diffraction peaks of the SiWA acid were not observed (Fig. 3A), suggesting a homogeneous distribution of Keggin's ions in the sol-gel network.^{16,17} However, it was interesting to notice that an increase in the amount of SiWA content led to an intensity increase of the diffraction band at 6.3° . Chen et al.³³ ascribed this band to the strong interaction between SiWA and silica. The intensity increase of this band suggested that the acid molecules acted as a surfactant for the precursor molecules, increasing the formation of silica clusters having the silsesquioxane structure. For membrane A, the low-angle diffraction peak was visible already for 20% SiWA content, and became the most intense peak for 40% SiWA content (Fig. 3B). The calculated correlation distance between clusters was 1.4 nm.

3. 3. Structural Studies: IR ATR Spectroscopic Characterisation of Membranes

IR ATR spectra of membranes: Membranes are considered as condensed PPGU and PDMSU precursors solidified due to hydrolysis and condensation reactions, which started after addition of SiWA acid and drastically modify the IR spectra of precursors, particularly in the region where the siloxane bands^{34,35} of PDMSU and the Si–O–C and C–O–C modes³⁶ of PPGU appeared (1200 – 1000 cm^{-1}) (Fig. 4). These modes have already been extensively investigated^{20,30,37} and will not be repeated here.

The other bands of PDMSU that can be seen in the spectra of membranes B and C are found at 1260 and 795 cm^{-1} , belonging to bending and rocking modes of Si–C in the $Si(CH_3)_2$ groups of poly(dimethylsiloxane) chains.³⁴ Moreover, the characteristic modes of Keggin anions (Fig. 5) could be observed, indicating the preservation of the Keggin units inside the hybrid composite. These bands are the stretching modes of Si–O_a in the central tetrahedra at 1017 and 918 cm^{-1} ,³⁸ asymmetric stretching modes of terminal $W = O_d$ at 978 cm^{-1} ,¹⁹ and asymmetric $W-O_b-W$ and $W-O_c-W$ modes at 891 and 778 cm^{-1} .^{13,38}

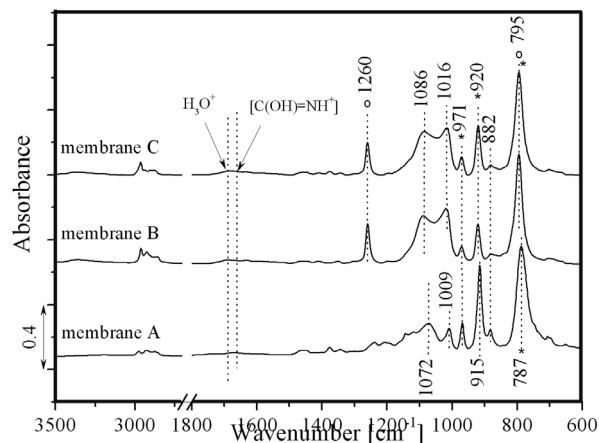


Fig. 4: IR ATR spectra of membranes A, B and C. For composition see Table 1. * denotes the vibrational modes of Keggin anions and ° of PDMSU precursor.

The urea bands in the spectral region from 1730 to 1250 cm^{-1} (Fig. 4) have to be considered in detail because they can provide information about the extent of protonation related to the conductivity. The urea groups are characterized by the amide I band ascribed to the $\nu(C=O)$ stretching mode (1730 – 1600 cm^{-1}), the amide II band corresponding to the in-plane N–H bending mode coupled with C–N stretching of the C–N–H group ($\delta(N-H) + (C-N)$)³⁹ between 1570 and 1515 cm^{-1} and finally, the

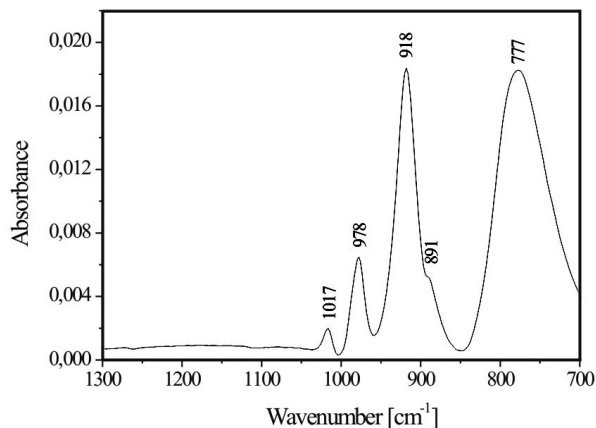


Fig. 5: IR ATR spectrum of heteropoly acid SiWA.

amide III band, defined as the C–N stretching mode^{40,41} (1350–1250 cm^{-1}). The characteristic property of amide I bands is that they are sensitive to hydrogen bonding, giving information about the nature and strength of H-bonding on C=O groups. On the other hand, the amide II bands offer information about the chain conformation and about the strength of the intermolecular hydrogen bonds.^{42–46} These facts were used to investigate the hydration of the membranes, their modification after the addition of various amounts of acid, and the assessment of the effect of autoclaving on the structure of the membranes.

In fact, two modes are of special importance; the band attributed to amidonium ions, i.e. $[\text{C}(\text{OH})=\text{NH}^+]$,²⁶ and the band of H_3O^+ ions.⁴⁷ The latter band has been actually detected for the heteropolyacids and its frequency has been substantiated from inelastic neutron spectra. Both bands were expected to appear in the spectra of membranes with relatively high acid content, as shown below.⁴⁸

IR ATR spectra of membrane A with various acid concentrations: The changes that occurred in the IR ATR spectra of membrane A with increase in the concentration of SiWA in the composite matrix are depicted in Fig. 6. It is evident that with increase in the concentration of acid from 20% to 80%, broad bands in the range 1750–1500 cm^{-1} developed, which can be ascribed to the presence of the amidonium $[\text{C}(\text{OH})=\text{NH}^+]$ ion.²⁶ This band was found for membrane A with 40% SiWA content at 1671 cm^{-1} (Fig. 6A), but moved to higher frequencies, i.e. to 1680 cm^{-1} , for more concentrated membranes (Fig. 8B). It clearly showed an increase in the number of protonated urea groups with increase in acid content. In addition, the presence of H_3O^+ ions in the membrane A with the highest SiWA contents (75%, 80%) could be detected through the appearance of the in-plane bending mode⁴⁷ at 1702 cm^{-1} . Increase in %SiWA to the membrane A also led to a disappearance of the amide II band at 1556 cm^{-1} , which also confirmed the formation of amidonium ions.

IR ATR spectra of membranes equilibrated at elevated temperature and pressure: The influence of water va-

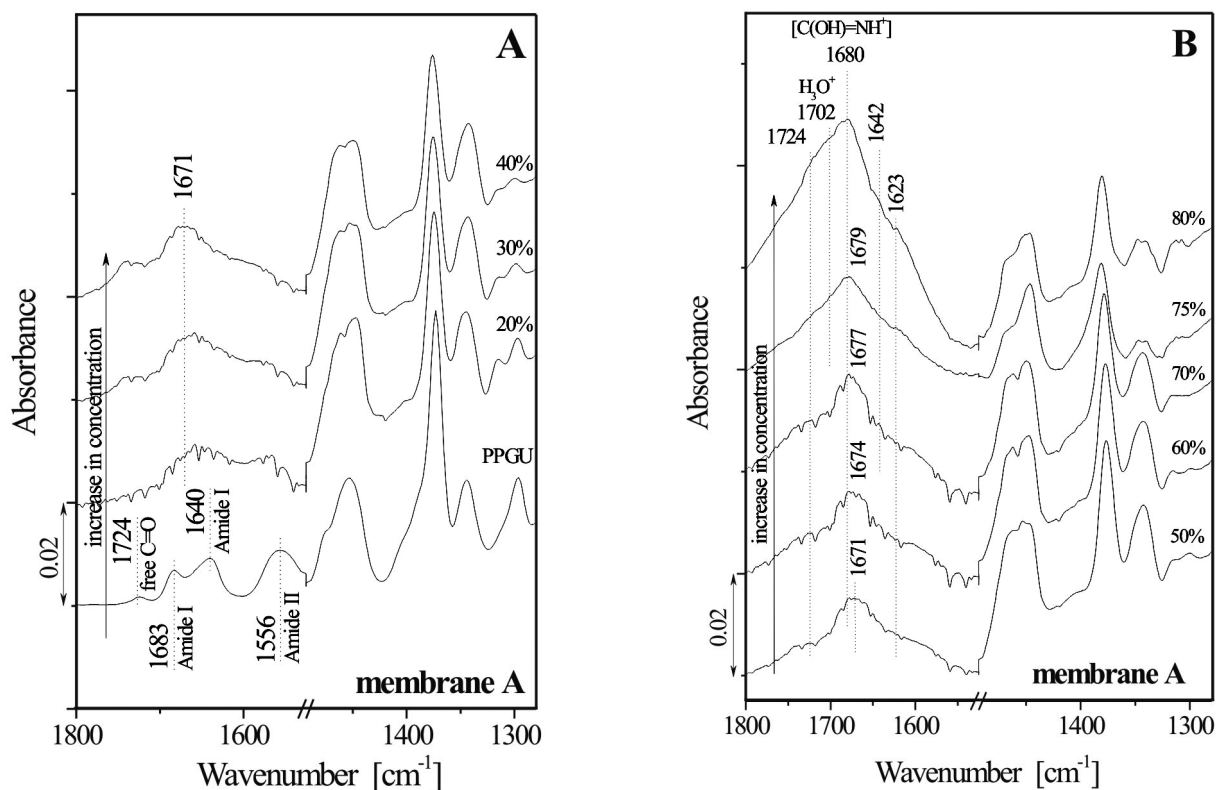


Fig. 6: IR ATR spectra of precursor PPGU (A) and membrane A with 20% to 80% SiWA acid content: A) 20–40 % and B) 50–80 %.

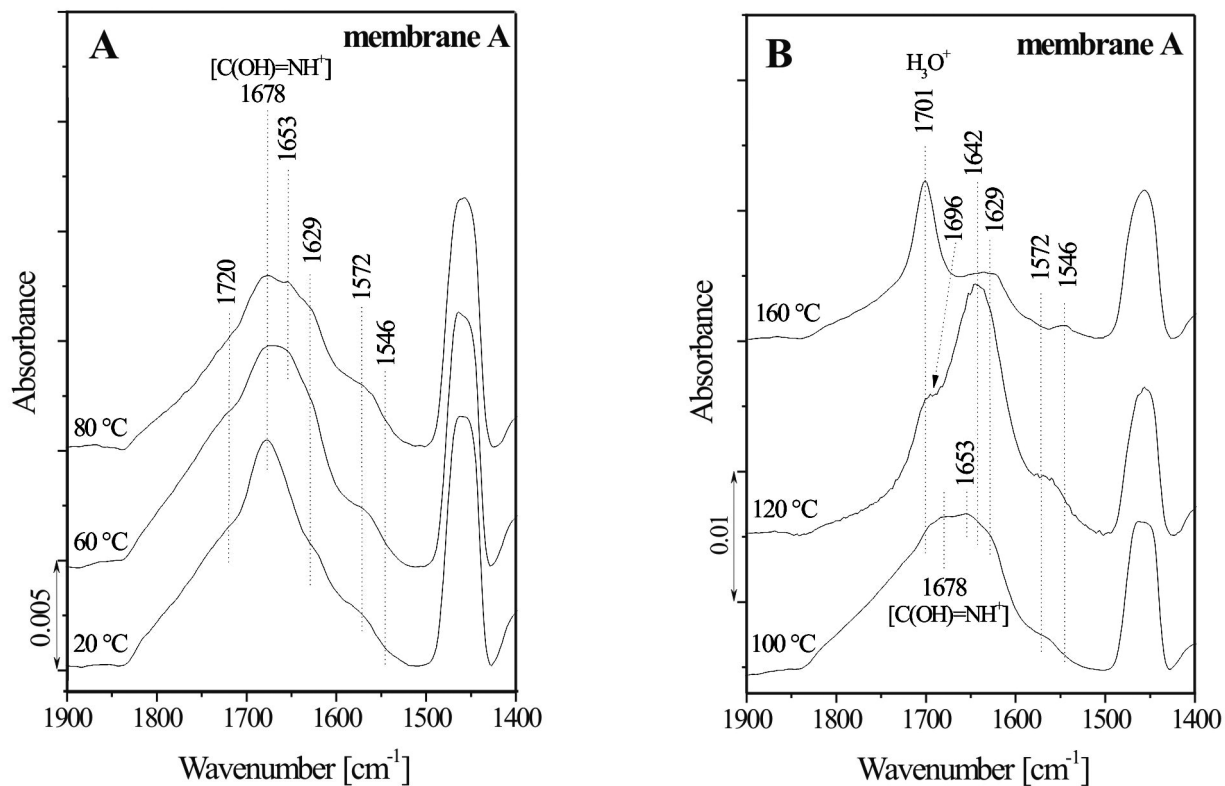


Fig. 7: IR ATR spectra of membrane A with 40% SiWA acid (Table 1): A) non-autoclaved (20 °C) and autoclaved at 60 and 80 °C and B) autoclaved at 100, 120 and 160 °C.

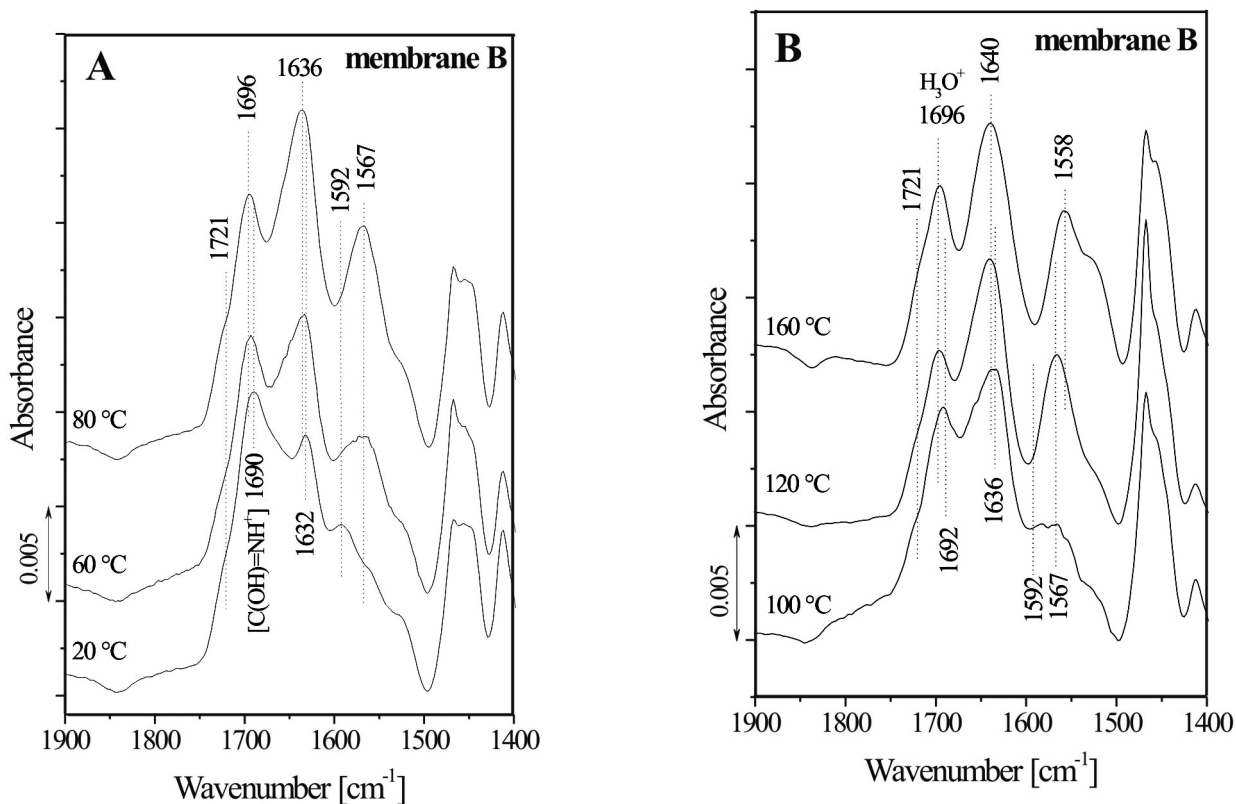


Fig. 8: IR ATR spectra of membrane B with 31% SiWA acid (Table 1): A) non-autoclaved (20 °C) and autoclaved at 60 and 80 °C and B) autoclaved at 100, 120 and 160 °C.

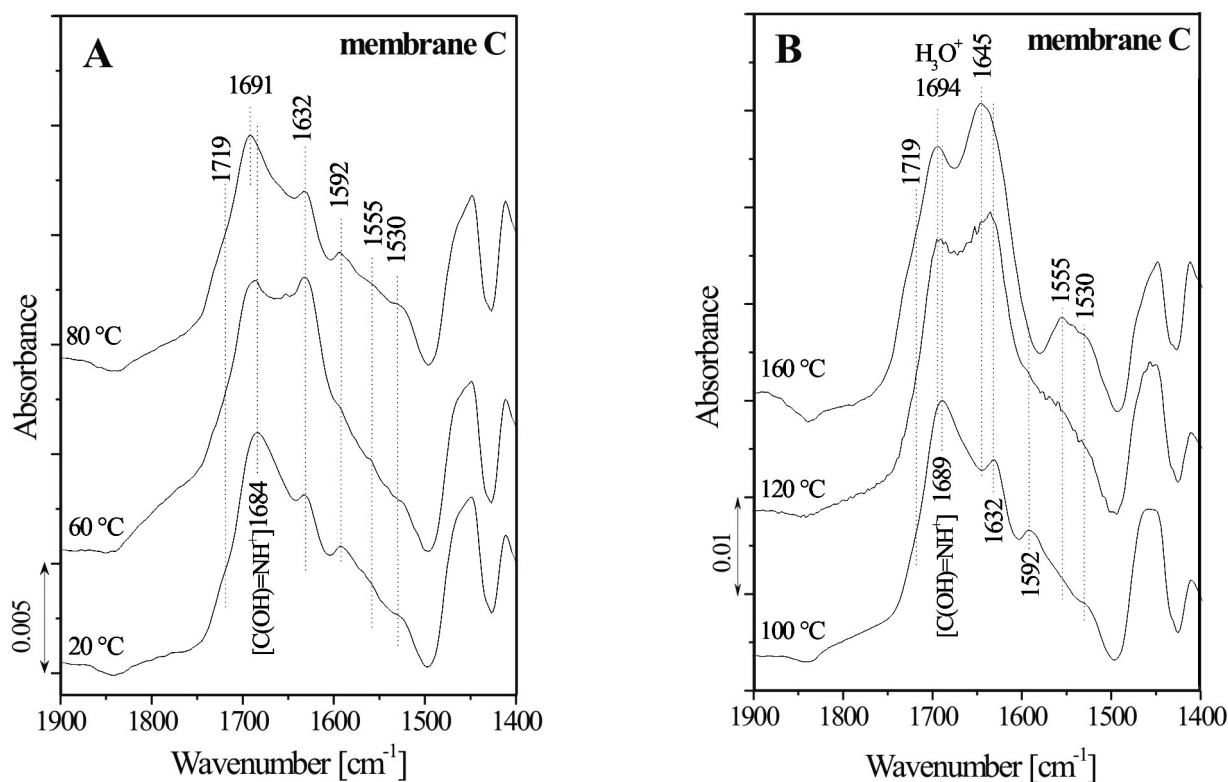


Fig. 9: IR ATR spectra of membrane C with 36% SiWA acid (Table 1): A) non-autoclaved (20 °C) and autoclaved at 60 and 80 °C and B) autoclaved at 100, 120 and 160 °C.

pour pressure at elevated temperature on the structure of proton conducting membranes A, B, C (Table 1) was tested by autoclaving samples in the temperature interval between 60–160 °C, followed by the measurement of their IR ATR spectra under ambient conditions (Figs. 7–9).

Membrane A: Up to an autoclaving temperature of 80 °C (Fig. 7A) the IR ATR spectra revealed the formation of a band at 1678 cm⁻¹ attributed to amidonium ions. At a temperature of 100 °C (Fig. B) formation of a shoulder ascribed to the in-plane deformational band of H₃O⁺ ions could be seen at 1701 cm⁻¹. The strong enhancement of the band³⁹ at 1642 cm⁻¹ for membrane A equilibrated at 120 °C signalled strong hydration, i.e. the increased presence of water molecules. The pronounced disappearance of amide I (1629 cm⁻¹), amide II (1572 cm⁻¹) and the band of amidonium ions in the spectrum of the sample equilibrated at 160 °C, together with the enhancement of the H₃O⁺ band at 1701 cm⁻¹, suggested degradation of the membrane A. Namely, the cleavage of urea groups led to a decrease in the number of conducting amidonium ions and a transfer of protons to water molecules, i.e. to abundant formation of H₃O⁺ species.

Membrane B: Already at ambient temperature the IR ATR spectra of PDMSU-based membrane B (Fig. 8) showed the presence of amidonium ions (1690 cm⁻¹) and the band at 1632 cm⁻¹, attributed to strong urea-urea associations (amide I). With increasing temperature of autoclaving the latter band gradually increased in intensity and shifted to higher frequencies, mainly as a consequence of the superposition of the water vibrational mode at 1640 cm⁻¹, indicating increased hydration of membrane B. The hydration was also reflected in the shift of the band of amidonium ions (1690 cm⁻¹) to higher frequencies (1696 cm⁻¹) due to partial transfer of protons from amidonium ions to water molecules (formation of H₃O⁺ ions). The appearance of the band at 1696 cm⁻¹ in the spectrum of membrane B equilibrated at 160 °C (Fig. 8B) revealed that both kinds of conductive ions were present in the polymer matrix, contrary to membrane A (degraded) (Fig. 7B), in which H₃O⁺ ions mainly remained at this temperature. It is important to note that membrane B contrary to membrane A remained stable and did not disintegrate at 160 °C; the amide II bands, which disappeared from the spectra of the membrane A (Fig. 7B) under these conditions were clearly seen in the corresponding spectra of the membrane B (Fig. 8B).

Membrane C: Fig. 9 shows the IR ATR spectra of membrane C, which is composed of the network formers of membrane A and B (Table 1). Accordingly, the evolution of the spectra followed those observed for membranes A and B. At ambient conditions, the band of amidonium ions appeared at 1684 cm⁻¹, an intermediate frequency value between those noted for membranes A and B. Amide I band at 1632 cm⁻¹ appeared with lower inten-

sity due to the lower PDMSU content of membrane C (Fig. 9A) with regard to membrane B (Fig. 8A). Up to the temperature of 100 °C, the spectra of membrane C showed a gradual intensity increase and a high-frequency shift (1684 to 1689 cm^{-1}) of the band of amidonium ions (Fig. 9). However, when membrane C was equilibrated at 120 °C, strong enhancement of the 1640 cm^{-1} band occurred, which implied strong hydration of the membrane C network (Fig. 9B), as already found for membrane B (Fig. 8B). Equilibration of membrane C at 160 °C indicated even stronger hydration without indication of the loss of structural integrity, which could be conceived from the loss of the amide II mode as noted for membrane A. The hydrophobic network of the added PDMSU considerably enhanced the thermal and pressure stability of membrane C. Nevertheless, the small blue frequency shift of the amidonium band from 1684 to 1694 cm^{-1} could be (as for membrane B) ascribed to the simultaneous presence of the conductive amidonium and H_3O^+ ions.

To conclude, the autoclaving of membranes A, B and C revealed that all the membranes were already protonated at room temperature, which we deduced from the presence of the band of the amidonium ion. When autoclaved the membrane A disintegrated at high temperatures and became saturated with H_3O^+ ions, but the structure of membrane B did not change and the conductive amidonium and H_3O^+ ions were present simultaneously. Membrane C (regarding its mixed composition) was more stable than membrane A and more elastic than membrane B. It seemed that the membrane C was the material of choice as regards use in a fuel cell. This we verified in the next step by measuring the temperature conductivity of membranes equilibrated at higher temperature and pressure.

3. 4. Conductivity Measurements of Membranes Equilibrated at Higher Temperatures and Autogenous Pressure

In the first step the conductivity variation of membranes having various contents of acid was determined (Fig. 10). Only the conductivity measurements of the membrane A are shown here because other membranes behaved similarly. Expectedly, the conductivity of the gelled samples increased with acid content but slightly dropped in the course of aging (2 days) at ambient temperature (Fig. 10). Then the bulk gels were equilibrated at ambient temperature in humid air (98%). Interestingly, those gels which contained more than 50% of acid showed an increase in the conductivity but the conductivity of the others dropped in the course of aging in humid air. Aging of bulk gels at a humid atmosphere prevented degradation of the gels, which remained in the form of monolithic gels.

The conductivity measurements confirmed that for practical use the acid content should be higher than 40% because such membranes showed the ability to increase their conductivity when equilibrated in a humid atmo-

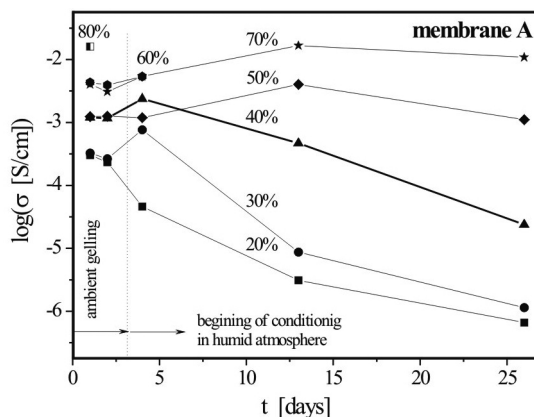


Fig. 10: Logarithmic dependence of conductivity on time of aging for bulk gels prepared according to the composition of membrane A (Table 1) with different %SiWA acid contents (20–70 %).

here. Accordingly, the membranes A, B and C were equilibrated at autogenous water pressure in the temperature interval from 30–160 °C and the conductivity recorded in analogy to the IR ATR spectroscopic measurements. At every measured temperature the time of equilibration was 15 min. For all membranes the conductivity increase with temperature was noted, reaching maximal values of about 10^{-2} S/cm (Fig. 11). The conductivity behaviour of membrane A revealed only slight increase in proton conductivity with increasing temperature. Its comparison with the IR ATR spectra of autoclaved membranes (Figs. 7–9) revealed that the high conductivity of membrane A could be attributed to the immediate formation and presence of amidonium ions. A loss of structural integrity of membrane A, as can also be deduced from TG measurements (Fig. 2), could be detected from the slight decrease of conductivity above 100 °C. However, the conductivity values remained high (i.e. 10^{-2} S/cm) due to the presence of H_3O^+ ions.

Membranes B and C did not show degradation of the polymeric network in the temperature region from 60–160

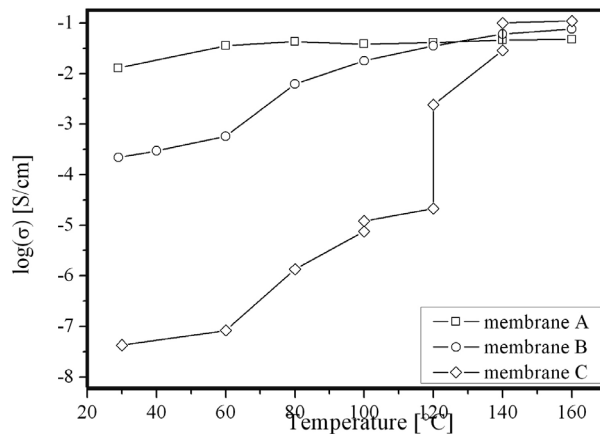


Fig. 11: Conductivity measurements of membranes A, B and C in the autoclave from room temperature up to 160 °C.

°C as inferred from the IR ATR spectra measurements (Figs. 8, 9). However, the spectra revealed the prevalence of amidonium ions below 100 °C, but the simultaneous presence of amidonium and H_3O^+ ions at higher temperatures. This effect could be correlated with the step in the conductivity curves noted in Fig. 11 for the same temperature range. The reason for the relatively abrupt increase in conductivity values we attribute to in forced hydration of the membranes, which contributes to formation of H_3O^+ ions. For instance, the conductivity of membrane C was $4.27 \cdot 10^{-8}$ S/cm at room temperature, but gradually increased up to 120 °C, then at this temperature promptly increased to $2.40 \cdot 10^{-3}$ S/cm as a consequence of hydration.

Surprisingly, at lower temperatures membrane B was more conductive than membrane C and the conductivity step from 60 to 100 °C was not as high as for membrane C (Fig. 11). This can be correlated with the results of TG analysis in air (Fig. 2) revealing that the lowest weight loss of 1.8% up to 120 °C was achieved for membrane C, while membrane B showed the weight loss of 3.4%. Obviously at ambient conditions the membrane B contains the highest amount of water, despite the lowest %SiWA content (31%) in the structure, which influences also its conductivity value through the formation of proton conductive species. The membrane C showed the most pronounced increase in conductivity values, and at the highest temperatures, i.e. 160 °C, reached the conductivity values similar to the other membranes. This indirectly proved that for membrane C the conductivity at the temperature of 160 °C could be attributed to the formation of H_3O^+ ions, as conceived also from the IR ATR spectra (Fig. 9).

4. Conclusions

Membranes for medium-temperature fuel cells were prepared on the basis of organic-inorganic sol-gel ureasil precursors with either poly(propylene glycol) (PPGU) or poly(dimethylsiloxane) (PDMSU) polymeric chains and heteropoly silicotungstic acid. Absolute values of the proton conductivity at room temperature were of the magnitude of 10^{-4} S/cm to 10^{-3} S/cm, increasing with acid content. Testing of the membranes in a “zero-gap” type autoclave cell at the equilibrium pressure of 6 bars and temperatures above 140 °C revealed that the conductivity increased to 10^{-1} S/cm, a value acceptable for applications in fuel cells. It was found that the membranes prepared from PDMSU hybrid precursor exhibit high proton conductivity at temperatures above 90 °C, good thermal stability up to 160 °C and good mechanical properties. An important disadvantage of PPGU membranes was noted in their thermal instability above 120 °C.

Infrared spectroscopy was found to be a useful tool for the investigation of the structure of such membranes. Namely, using IR ATR spectroscopy we followed the presence of amidonium ($\text{C}(\text{OH})=\text{NH}^+$) and H_3O^+ ions in the

matrix of sol-gel membranes autoclaved at high temperatures. It was shown that autoclaving led predominantly to protonation of urea groups at lower temperatures, while after significant hydration of the membranes, hydronium ions formed as well.

5. Acknowledgement

This work was performed under EU project APOL-LON, contract no. ENK5-CT-201-00572. J. Vince thanks the Slovenian Research Agency for Ph.D. grant. Authors thank dr. Romana Cerc Korošec from University of Ljubljana, Faculty of Chemistry and Chemical Technology for thermogravimetric measurements.

6. References

1. K. D. Kreuer, *J. Membr. Sci.* **2001**, *185*, 29–39.
2. B. Tazi, O. Savadogo, *Electrochim. Acta* **2000**, *45*, 4329–4339.
3. J. Livage, *Current Opinion Solid State Mater. Sci.* **1997**, *2*, 132–138.
4. J. Livage, F. Beteille, C. Roux, M. Chatry, P. Davidson, *Acta Materialia* **1998**, *46*, 743–750.
5. J. D. MacKenzie, *J. Sol-Gel Sci. Technol.* **1994**, *2*, 81–86.
6. B. D. Ghosh, K. F. Lott, J. E. Ritchie, *Chem. Mater.* **2005**, *17*, 661–669.
7. B. D. Ghosh, K. F. Lott, J. E. Ritchie, *Chem. Mater.* **2006**, *18*, 504–509.
8. J.-D. Kim, I. Honma, *Solid State Ionics* **2005**, *176*, 547–552.
9. I. Honma, S. Hirakawa, K. Yamada, J.M. Bae, *Solid State Ionics* **1999**, *118*, 29–36.
10. I. Honma, Y. Takeda, J. M. Bae, *Solid State Ionics* **1999**, *120*, 255–264.
11. I. Honma, S. Nomura, H. Nakajima, *J. Membr. Sci.* **2001**, *185*, 83–94.
12. U. Lavrenčič Štangar, N. Grošelj, B. Orel, A. Schmitz, P. Colombar, *Solid State Ionics* **2001**, *145*, 109–118.
13. M. J. Janik, K. A. Campbell, B. B. Bardin, R. J. Davis, M. Neurock, *Appl. Catal. A* **2003**, *256*, 51–68.
14. U. B. Mioč, S. K. Milonjić, D. Malović, V. Stamenković, P. Colombar, M. M. Mitrović, R. Dimitrijević, *Solid State Ionics* **1997**, *97*, 239–246.
15. U. B. Mioč, S. K. Milonjić, V. Stamenković, M. Radojević, P. Colombar, M. M. Mitrović, R. Dimitrijević, *Solid State Ionics* **1999**, *125*, 417–424.
16. P. Staiti, S. Freni, S. Hočevar, *J. Power Sources* **1999**, *79*, 250–255.
17. P. Staiti, M. Minutoli, S. Hočevar, *J. Power Sources* **2000**, *90*, 231–235.
18. S. Shanmugam, B. Viswanathan, T. K. Varadarajan, *J. Membr. Sci.* **2006**, *275*, 105–109.
19. X. Zhao, H.-M. Xiong, W. Xu, J.-S. Chen, *Mater. Chem. Phys.* **2003**, *80*, 537–540.

